

Artificial Neural Network Classification of Asteroids

A. Misra¹ and S. Bus²

Institute for Astronomy, University of Hawaii, Hilo, HI 96720

ABSTRACT

There are currently only a few thousand asteroids with known classifications. Our aim is to increase this number to over 20,000 by classifying asteroids identified in the Sloan Digital Sky Survey (SDSS) Moving Object Catalogue using an artificial neural network that has been developed using the Neural Network Toolbox in Matlab. With this neural network, we are able to provide classifications for 22,847 asteroids based on normalized reflectances derived from the g' , r' , i' , and z' SDSS magnitudes. The neural network was trained using a combination of previously classified asteroids, asteroids from known dynamical families, and asteroids we classified by hand from the SDSS reflectances. The previously classified asteroids were from the Small Main-Belt Asteroid Spectroscopic Survey (SMASS) and the Small Solar System Objects Spectroscopic Survey (S3OS2). Asteroids were divided into 13 spectral classes (T, D, B, C, X, K, S, L, A, R, Q, V and O), based on the previous taxonomies of Tholen (1984) and Bus and Binzel (2002). A major advantage of the neural network approach is that it generates a set of possible classifications for each asteroid, along with associated probabilities that emulate the continuum between classes observed in asteroid taxonomy. Our neural network solution can be applied to any new asteroid observations made in the g' , r' , i' , z' system. We anticipate that this network and any supporting algorithms will be made publicly available in the near future via the world wide web. We will present a description of this artificial neural network and the resulting classifications as well as a discussion of its accuracy and limitations. This work was conducted through a Research Experience for Undergraduates (REU) position at the University of Hawaii's Institute for Astronomy, funded by the NSF.

Subject headings: asteroids, asteroid families, SDSS, SMASS, S³OS², asteroid taxonomy

1. Introduction

Knowing the composition of the overall population of asteroids is essential to modeling Solar System origins and evolution. Taxonomic classifications, while not precise mineralogy, do give some indication of the composition of asteroids. Perhaps more importantly, taxonomy provides an easy way of conveying information about asteroids with only a handful of letters. Previously there have only been a few thousand classified asteroids. By comparison, there are hundreds of thousands of asteroids with known orbital elements. How-

ever, with large scale photometric surveys such as the Sloan Digital Sky Survey (SDSS), it is possible to classify an order of magnitude more asteroids than what is currently known. We have done this by training an artificial neural network to classify asteroids from the SDSS Moving Object Catalogue (SDSS MOC) based on the g' , r' , i' , and z' magnitudes from the SDSS.

Previous asteroid classifications have usually placed a single, unique classification to asteroids. The approach we have taken is to give each asteroid a probability of belonging to one class or another. This strategy embraces the idea that the different types of asteroids form a continuum in spectral parameter spaces. Unlike with stellar classifications, there are not definite boundaries between different asteroid classes.

¹Undergraduate, Case Western Reserve University and REU student at IfA Hilo during the summer of 2008.

²Associate Astronomer, Institute for Astronomy at University of Hawaii-Hilo.

We chose to use an artificial neural network to classify these asteroids because of the convenience of having a computer program to classify asteroids and because of the pattern recognition abilities of these non-linear algorithms. Artificial neural networks can be trained to recognize patterns by using training data sets and then can use those patterns and apply them to new data by running a simulation. Additionally, a neural network lends itself to emulating the continuum of asteroid classes. The neural network produces a probability distribution for each asteroid so that there are no absolute classifications. All these factors make neural networks an appealing approach to the subject of asteroid classifications on a large scale.

One anticipated use of this work is that it is possible to use our methods and algorithms for any set of g , r , i , and z magnitudes and get an asteroid classification. This could be very useful considering that future all-sky surveys such as the Panoramic Survey Telescope and Rapid Response System (Pan-STARRS) and the Large Synoptic Survey Telescope (LSST) will likely use the Sloan filter set, allowing our neural network to be used with any asteroid data from these and other surveys.

2. Artificial Neural Networks

Artificial neural networks were inspired by biological nervous systems. The network contains many simple elements that are interconnected into one large, complicated system. The overall function of the network is determined by the connections between the elements and the weights between them.

The most basic element of a neural network is a neuron. A neuron takes in a scalar or vector input, multiplies it by a vector or scalar weight, and adds on a scalar bias. The result of that is then inputted into a transfer function. The output of the transfer function is either sent into another neuron (or layer of neurons) or is outputted as the result of the neural network. By adjusting the weights, biases, and transfer functions a neural network can be trained to give some desired result.

While there are many different types of neural networks, we utilized a multi-layer feed-forward backpropagation network. This type of network

feeds training data through multiple layers of neurons until the error between the neural network output and the expected training result reaches a low enough value. We used a network with two layers, meaning that our input data was sent into one set of neurons (a layer), and the output from those neurons were sent into another layer before the network gave the result. We used two different training sets with slightly different structures. The first network's first layer had 20 neurons, and the second layer had 13 neurons, one neuron for each of the 13 taxonomic asteroid classes we defined. The transfer functions used were a tangent sigmoid function for the first layer and a logarithmic sigmoid function for the second layer. The difference between the network for the first training set and the second training set was that the second network utilized 25 neurons in the first layer. We trained both networks over 10,000 iterations using the training data, which will be discussed in the next section.

3. Training Data

The training data for the neural network consisted of a set of classified asteroids that the neural network could use to determine patterns. As previously stated, we used two different training sets.

The first training set contained asteroids from multiple sources. First we found previously published taxonomic classifications from SMASS (1) and S³O² (7). There were 249 of these asteroids that were also contained in the SDSS MOC. These two surveys were based on the Bus and Binzel taxonomy, presented in their 2002 paper. This system recognized 26 different taxonomic classes. However, with only the SDSS magnitudes to classify asteroids we were not able to differentiate between all of their distinct classes, resulting in a more slimmed down version of the Bus and Binzel taxonomy which contained 13 classes. The differences between the two different systems are shown in Table 1. For example, the Ch class was absorbed into the C class because the difference between a typical Ch and a typical C asteroid, along with the strength of the 0.7 μ m absorption feature, is typically within the expected error and cannot be differentiated based on the Sloan bandpasses (Vilas 2005).

Another source of training set objects was as-

teroid families. The SDSS MOC not only found asteroids, it also compared these objects to asteroids with known orbital elements. All the SDSS asteroids we classified also have known proper semi-major axes, eccentricities, and inclinations. Using this orbital data, we were able to find potential asteroid families (Bus 2009, in progress). These were compared to known families and many matches were found, along with several possible new families. All the asteroids within a family are expected to have similar compositions, and therefore should have approximately the same spectra Cellion et al (2). This meant that once we knew that a group of asteroids was from the same family, we assumed they all had the same classification. Once we determined the classifications for the families, both from our own examination of the data and comparison to previous work, we took a subset from each family and added it to the training set. The total training set contained 534 asteroids from the families.

The last source of asteroids for the training set was hand-classified asteroids from the SDSS data set. Certain asteroid classes, such as the Q, R, A, T, and O classes, had very few known members and no known families that we could use. Therefore we manually added asteroids of these types by examining individual asteroids in the overall data set based on inspection of their spectral reflectances and their locations in spectral parameter space, which are based on principal component analysis. This provided us with 107 additional asteroids. Later this was expanded to include more asteroids in well-defined classes, such as the C and S classes, in order to provide more balance in the training set and also to strengthen the neural networks classification abilities. Adding asteroids from these classes added 897 asteroids (all of which were concentrated around specific points in principal component space).

The second training set was the culmination of several different attempts at alternate training sets. We tried using training sets based on average asteroid spectra taken from Bus & Binzel (1). We also tried training only with a solid core of asteroids for each class (with the core being defined as the center of each class in principal component space). None of these attempts worked as successfully as the original, so in the end we went through a set of approximately 586 asteroids and classi-

fied them by eye, based solely on their spectral reflectances calculated from the Sloan magnitudes and created a training set from our classifications. This was the second training set we used to determine the asteroid classifications. Plots of the two training sets in principal component space can be found in Figure 5 on page 18.

4. Data Analysis

The SDSS data was part of the third release of the SDSS MOC (5). We used only entries that had been linked to known asteroids and that had relatively low errors associated with each of the g' , r' , i' , and z' magnitudes. We chose not to use the u' magnitudes because of the large errors on these measurements that are typical relative to the other filters. We also used the v magnitude, which is calculated from the g and r magnitudes and provided in the MOC.

We were able to calculate four different colors from these five magnitudes. We found c_{g-v} , c_{v-r} , c_{v-i} , and c_{v-z} using the following equations, which are modified from Ivezić et al (4) in order to account for the use of the V magnitude:

$$c_{g-v} = g - v - .2720 \quad (1a)$$

$$c_{v-r} = v - r - .1780 \quad (1b)$$

$$c_{v-i} = v - i - .2780 \quad (1c)$$

$$c_{v-z} = v - z - .3180 \quad (1d)$$

These four colors can then be used to calculate the relative reflectances for each band:

$$F_g = 10^{-.4*c_{g-v}} \quad (2a)$$

$$F_r = 10^{.4*c_{v-r}} \quad (2b)$$

$$F_i = 10^{.4*c_{v-i}} \quad (2c)$$

$$F_z = 10^{.4*c_{v-z}} \quad (2d)$$

These relative reflectances (F_g , F_i , F_r , and F_z) were what we used to determine the spectral classifications of the asteroids.

We also conducted principal component analysis on these relative reflectances. While these numbers were not used as part of the neural network, they did prove convenient for plotting the asteroids in two-dimensional space. Principal component analysis is a technique that can be used to reduce the dimensionality of a data set. The general idea behind this is to project the data onto

a small number of axes such that the maximum amount of the original data’s variance is preserved. Usually when principal component analysis is performed on asteroid spectra the first component of the analysis is very closely correlated to the slope. Therefore, we manually took out the slope from the relative reflectances. We calculated the slope by fitting a line to each set of four reflectances. These fits were constrained such that the value at $.55 \mu\text{m}$ fixed at 1, in order to keep the point that corresponds to the V filter the same for all spectra. Once this best-fit line was calculated we subtracted the slope of the line from the data, and performed principal component analysis on the residual reflectance values. Finally, in order to make the second principal component score close to what was computed in previous studies, i.e. Bus & Binzel (1), we adjusted the second principal component score by adding a constant and then scaling by taking the natural logarithm.

5. Results

Once the neural network was trained using the aforementioned training sets, we were able to simulate the network with the reflectances from the entirety of the SDSS MOC. After eliminating asteroids with large uncertainties in the SDSS magnitudes, we were left with 22,847 asteroids. The neural network output for each asteroid is similar to a probability distribution. It gives a probability of an asteroid belonging to each of the thirteen taxonomic classes used. In this paper, we will be looking mostly at the highest probability of each asteroid, and evaluating how strong (high probability) or weak (low probability) the classification is.

To get these results, we used the weights and biases calculated by the neural network. To classify an asteroid with four relative reflectances, we used the formula that the neural network would have used:

$$result = \text{logsig}(lw * \text{tansig}(iw * ref + b1) + b2) \quad (3)$$

where ref is the relative reflectances of an asteroid, lw is the layer weight, iw is the input weight, $b1$ is the bias for the input layer, and $b2$ is the bias for the second layer. The values for needed matrices and vectors can be found in tables 3, 4, 5, 6, 7 and 8. The functions logsig and tansig

are the logarithmic sigmoid and tangent sigmoid, respectively. The tangent sigmoid function is the inverse tangent normalized to have a maximum and minimum of ± 1 .

We used this equation with both training sets, normalized the results, and then took the mean of the two different resulting matrices to get our final results.

The total number of asteroids classified into each type is shown in table 2.

To more easily view the results, we took a random sample of 1000 asteroids from the results, and plotted them in principal component space. We did this for each training set, and for the final results. These plots can be seen in Figures 7 and 8.

6. Evaluation of the Neural Network

We evaluated the performance of the neural network by comparing the network outputs to known classifications, simulating the network with average spectra, and looking at the results in principal component space.

6.1. Simulation of Average Spectra

We used data from Bus & Binzel (1) to create average spectra for every asteroid class. We then used the neural network to classify these averages. The results were very good. For the thirteen spectral classes we used, most of the average spectra were classified correctly with probabilities over 70%. Some of the average spectra were not classified very accurately, such as with the K and T spectra. The T’s are not considered to be a very strong class to begin with, and the difference between a K and an S, which is what the K spectrum was primarily classified as, is quite small, so these results are still promising.

As for the other classes, the spectra were classified correctly with probabilities of 70% or higher, even for some of the weakest classes, such as the R and Q classes that have very few known members based on previous spectral surveys. Many of the other classes, such as the B, C, S, and V classes, were classified with even higher probabilities.

6.2. Principal Component Plots

Another way we evaluated the results of the neural network is to look at the results in principal component space. We plotted slope versus principal component 2 and each class clearly fell into a distinct group. A graph of this can be seen in Figure 1 on page 14. This figure shows that the different classes form distinct groups, as is expected from previous work in this area. We also looked at a random sample of 1000 asteroids from the results to see a clearer picture of the boundaries between the asteroid classes. From this graph it is clear that not only do the classifications match the expected results in principal component space, they also agree with the idea that asteroid classes form a continuum in spectral parameter space, where the boundaries between these taxonomic classes are not well-defined.

Additionally, we looked at contour plots of probabilities for each class. We divided the asteroids into groups according to how high the probability was for each type of asteroid, and then plotted the results in principal component space. An example of this is seen in Figure 6 on page 19. The plot shows where the V type asteroids are found in PC space, along with the strength of the V classifications. The figure shows that the V types are found in the bottom left corner, which is expected, and that there are many very strong V classifications from the neural network. Additionally, once again it is clear that there is a region where the probabilities of V-type classifications is not very high.

As for the other classes, the D, B, C, X, K, S and L types, along with the V types, have many strong classifications in a well-defined region of PC space. The T, A, R, Q and O types are not necessarily incorrectly classified, but there are far fewer asteroids in these groups, and for the T, R and Q classes, there are not many strong classifications.

6.3. Orbital Elements

We also looked at each class in orbital element space. We were able to find families, such as the Vesta family by plotting semi-major axis versus inclination. While we did not perform an extensive study on the orbital data for each class, the data did confirm that our results were accurate.

Within the Vesta family, many of the asteroids

were classified as both R and Q types. While originally concerned, we later discovered that there is significant spectral disparity within the Vesta family. Therefore, not every asteroid was classified as V type. The orbital elements plots can be found in Figure 3 on page 16. Also, a graph of the spectra for the V and R types asteroids within the Vesta core is in Figure 4 on page 17.

7. Conclusions

The neural network does a fairly good job of classifying asteroids based on the g' , r' , i' and z' magnitudes from SDSS. Over 90% of the asteroids from the SDSS MOC were classified with greater than a 50% probability, meaning that the neural network provides a relatively good estimation of an asteroid's taxonomic classification.

However, the neural network works better for some classes than others. The results for the V class are very promising. The network accurately classified the average V-type and the V-type from the test portion of the training set. Also, there is a large number of very strongly classified V-type asteroids. As shown in Table 2, there were over 1000 V-types classified by the network.

The neural network's main weakness seems to be in finding Q, R, and T type asteroids. These asteroids are fairly rare, making it harder to develop patterns for these classes in the training sets. However, the neural network performs well with the other types of asteroids, and at the very least can easily provide a classification for any input of the g' , r' , i' and z' SDSS magnitudes.

One very positive feature about the results is that not only do the primary classifications seem correct, but also the results help to reinforce the continuum between the different classes. With a data set so large, not every asteroid is going to fall clearly into one class or another, and there are some spectra that did not resemble anything found in current taxonomic systems. Perhaps more significant than the fact that 90% of the asteroids were classified with probabilities better than 50% is that 10% of the asteroids were not. For asteroids that lie in regions of spectra space between classes or for asteroids with unique spectra, the probabilities should not be very high. The use of a neural network has allowed us to accommodate this fact by assigning probabilities instead of ab-

solute classifications.

This system also has future uses. Pan-Starrs and LSST are most likely going to use filter sets that uses the g',r',i' and z' bandpasses, meaning that this neural network classification system can be used on any asteroids observed with those surveys.

Funding for the creation and distribution of the SDSS Archive has been provided by the Alfred P. Sloan Foundation, the Participating Institutions, the National Aeronautics and Space Administration, the National Science Foundation, the U.S. Department of Energy, the Japanese Monbukagakusho, and the Max Planck Society. The SDSS Web site is <http://www.sdss.org/>.

The SDSS is managed by the Astrophysical Research Consortium (ARC) for the Participating Institutions. The Participating Institutions are The University of Chicago, Fermilab, the Institute for Advanced Study, the Japan Participation Group, The Johns Hopkins University, Los Alamos National Laboratory, the Max-Planck-Institute for Astronomy (MPIA), the Max-Planck-Institute for Astrophysics (MPA), New Mexico State University, University of Pittsburgh, Princeton University, the United States Naval Observatory, and the University of Washington.

The authors wish to recognize and acknowledge the very significant cultural role and reverence that the summit of Mauna Kea has always had within the indigenous Hawaiian community. We are most fortunate to have the opportunity to conduct observations from this sacred mountain.

REFERENCES

Bus, S. & Binzel, R. P. 2002, *Icarus*, 158, 106-177
Cellino, A, 2002, *Asteroids III*, 633-643
Cox, E. S. et al, 1994, *Journal of Geophysical Research*, 99, E5, 10847-10865
Ivezic, Z. et al, 2001, *AJ*, 122, 2749-2784
Ivezic, Z. et al, 2002, *astro-ph/0208099*
Ivezic, Z. et al, 2002, *AJ*, 124, 2943-2948
Lazzaro, D et al, 2004, *Icarus*, 172, 179-220

holen, D. J. & Barucci, M. A., 1989, *Asteroids II*, 298-315

Vilas, F, 2005, *Lunar and Planetary Science XXXVI*, 2033

arell, J. & Lagerkvist, C. I., 2007, *A&A*, 467, 749-752

This 2-column preprint was prepared with the AAS L^AT_EX macros v5.2.

TABLE 1
 OUTLINE OF OUR TAXONOMIC SYSTEM, AS COMPARED TO THE BUS AND BINZEL SYSTEM

Bus and Binzel	Revised System for SDSS data
A	A
B	B
C	C
Cb	$\frac{1}{2}B$ $\frac{1}{2}C$
Cg	C
Cgh	C
Ch	C
D	D
K	K
L	L
Ld	L
O	O
Q	Q
R	R
S	S
Sa	$\frac{1}{2}S$ $\frac{1}{2}A$
Sk	$\frac{1}{2}S$ $\frac{1}{2}K$
Sl	$\frac{1}{2}S$ $\frac{1}{2}L$
Sq	$\frac{1}{2}S$ $\frac{1}{2}Q$
Sr	$\frac{1}{2}S$ $\frac{1}{2}R$
T	T
V	V
X	X
Xc	$\frac{1}{2}X$ $\frac{1}{2}C$
Xk	$\frac{1}{2}X$ $\frac{1}{2}K$
Xe	$\frac{1}{2}X$ $\frac{1}{2}K$

TABLE 2
 NUMBER OF ASTEROIDS CLASSIFIED INTO EACH ASTEROID TYPE. ALSO, THIS TABLE SHOWS THE PERCENTAGE OF ASTEROIDS IN EACH TYPE, BASED ON BOTH THE NEURAL NETWORK RESULTS AND PREVIOUS RESULTS FROM BUS & BINZEL (1).

Statistic	T	D	B	C	X	K	S	L	A	R	Q	V	O
Neural Network Results	396	909	1804	3011	2381	1637	7399	2739	356	611	485	989	130
Percentage	1.74	3.98	7.90	13.18	10.42	7.16	32.38	11.99	1.56	2.67	2.12	4.33	.57
Training Set 1	60	154	141	222	1216	239	351	250	42	60	27	164	36
Training Set 1 %	3.33	8.53	6.53	10.46	11.28	12.26	18.56	12.80	1.61	2.68	1.16	8.88	1.93
Training Set 2	6.50	49.45	43.30	88.95	84.35	50.75	107.5	42.85	19.05	17.40	21.90	41.70	12.30
Training Set 2 %	1.11	8.44	7.39	15.18	14.39	8.66	18.34	7.31	3.25	2.97	3.74	7.12	2.10

TABLE 3

MATRIX FOR THE INPUT WEIGHTS FOR THE FIRST TRAINING SET'S NEURAL NETWORK NEEDED TO CALCULATE THE RESULT FOR AN ASTEROID'S FOUR RELATIVE REFLECTANCES.

Input Weights			
-19.1320	-2.3470	0.1742	3.0421
10.5720	14.0960	-2.8977	4.3701
-10.8020	-1.0018	-2.8798	1.0226
-19.3890	10.9100	2.5078	-0.4979
-13.3510	-4.8868	-6.7208	-4.1562
-6.3159	-10.8080	7.0112	4.4786
0.5326	1.7377	-10.0380	-5.3177
-11.3170	12.1800	6.2651	3.7456
-17.6870	-12.5270	2.5301	1.2932
2.6971	-15.1440	-10.3830	-0.6546
-5.4241	-1.2240	7.6595	-5.1017
-8.0361	17.0730	-6.0201	-0.7400
6.2013	15.4260	-8.0820	2.7102
2.7891	-22.0560	-4.6573	-1.4992
12.6590	11.3580	-6.9979	-3.0725
-4.0609	9.6895	4.2445	5.3477
-19.6100	-11.7730	-12.3930	-3.2268
17.0320	-6.4581	9.3197	0.4493
-10.8700	16.2030	4.4644	-4.8809
-13.2550	11.4170	-4.4041	3.4994

TABLE 4

MATRIX FOR THE LAYER WEIGHTS FOR THE FIRST TRAINING SET'S NEURAL NETWORK NEED TO CALCULATE THE RESULT FOR AN ASTEROID'S FOUR RELATIVE REFLECTANCES.

		Layer Weights																			
-1.83850	32.2880	-1.2059	4.8926	2.7939	0.9417	1.4576	-1.0544	29.7540	10.3160	-0.0911	-15.0070	-0.1232	0.9604	-52.2990	-59.3740	0.3169	-1.9724	0.5995	16.6480		
-1.2355	279.2300	-1.3620	29.4770	-1.9889	-0.2470	1.5810	0.1846	-38.8380	-9.4407	0.6200	1.5226	3.2492	0.7257	36.7540	3.9335	0.3102	-2.5401	-0.2690	-76.8480		
-1.0268	-11.5080	-0.1905	-3.2883	-1.0927	-3.5077	1.1215	-2.4334	1.3699	-0.6369	-6.3801	0.4683	3.2492	0.7257	-1.4873	-0.0655	16.8560	-0.0793	1.1693	1.1735		
8.4441	-9.7663	-4.3292	4.3195	8.9140	7.5535	3.7172	-8.5687	0.6631	1.5276	-10.2150	-2.9368	-11.1610	0.2710	4.2424	0.1374	1.6162	-3.9223	2.1436	4.5879		
6.9454	-9.7498	-0.7332	-0.5335	-12.4010	14.4070	0.8996	5.3753	0.3540	7.7757	-4.5403	-5.3720	-5.1788	0.1251	23.7480	-0.0061	8.1375	-2.4305	-0.3601	12.4180		
0.2104	-20.3200	-5.9741	3.1222	11.5300	1.9512	5.8158	8.2128	6.1074	15.0210	-17.3460	-8.9272	-8.3389	1.3118	-23.2840	-7.8113	1.7754	-6.0061	1.1557	8.7646		
-0.8135	-29.6680	-9.5426	-0.3378	2.7667	-3.7672	2.2372	0.3698	48.1880	-6.2571	-14.1570	-0.7556	-3.9819	8.9553	8.8305	-6.6614	0.5107	-3.5442	-4.5276	-0.0491		
-0.2957	-83.1390	-6.0607	-12.7330	-4.4540	0.8199	5.7480	1.2982	4.6849	2.2004	-26.6780	-0.3385	-17.3950	-1.1761	-2.6966	3.9635	4.5024	-5.6981	-1.7578	8.9442		
-0.7495	-9.5707	-6.4621	-3.8956	-13.4710	0.4027	6.0173	0.2880	-0.3715	0.8938	28.9040	-2.1355	42.4860	-0.1958	-4.9876	-13.2650	3.8415	-24.7140	-4.5960	-1.1413		
-1.0905	-0.6885	-3.2846	-3.1381	-1.1964	7.2697	3.9056	0.7469	3.3773	-0.2442	10.9770	-7.2122	4.1235	-0.3263	16.4780	-0.6646	7.0567	-6.4391	-5.4373	7.8086		
0.9927	-27.2740	-6.8230	1.8706	2.1289	5.7683	6.8413	1.8211	18.5320	1.1444	-5.0189	-0.6917	-4.1235	-2.3513	16.4780	-0.3968	7.0567	-6.4391	-5.4373	-0.7278		
-16.0410	1.4472	-2.9102	7.1460	6.5381	3.7283	1.7257	6.0182	-21.3070	-1.8630	5.9104	0.1065	9.4196	4.9555	-11.7630	0.2003	2.6966	-1.2925	7.4427	-3.5520		
6.5941	-12.8840	-2.1028	-2.4946	-0.4893	-4.5272	0.5018	-7.0596	28.3690	70.4790	25.6900	1.0540	-2.9938	-30.5500	-0.7209	0.4229	0.4854	-1.9859	0.6781	6.6913		

TABLE 5

BIAS VECTORS FOR THE FIRST TRAINING SET'S NEURAL NETWORK NEEDED TO CALCULATE THE RESULTS FOR AN ASTEROID'S FOUR RELATIVE REFLECTANCES.

B1	B2
18.3430	-4.1574
-27.1480	1.2201
36.3810	1.5488
5.0516	-1.7618
30.1600	-2.4580
5.9690	-6.2356
-9.6362	-8.3198
-12.1690	-4.7525
25.2970	-3.6809
26.3110	-5.0758
2.5732	-5.3079
19.0980	-4.5044
-14.9990	-4.2646
28.4780	...
-12.7500	...
-18.6730	...
25.5670	...
2.6245	...
-9.8636	...
-0.0428	...

TABLE 6
INPUT WEIGHTS FOR THE SECOND TRAINING SET'S NEURAL NETWORK.

Input Weights			
6.0903	-20.02	6.053	-2.8315
2.1253	6.296	8.2403	7.1578
1.8978	8.941	-5.7742	-10.495
10.958	9.7077	-6.6312	-8.1932
-15.373	-6.7123	-1.2887	5.6194
14.386	18.032	-4.9885	-1.0621
-20.686	1.1959	4.9317	-2.7822
-6.5171	15.557	8.032	-4.2625
-9.927	-13.892	7.7646	4.2232
15.335	-10.912	5.288	-3.3498
-17.087	11.827	-6.1095	-2.3787
3.2614	17.495	4.8217	5.2035
6.0025	14.813	-11.444	-0.2785
5.1808	-11.114	-11.735	4.8518
14.687	-14.556	-8.8976	4.4494
-19.374	8.4353	-11.895	-2.1686
11.608	11.395	2.1165	-5.6704
1.2259	-12.231	-13.142	0.10297
10.815	-6.6653	11.113	-1.5737
-14.102	-14.808	0.2958	3.6998
1.5552	14.713	10.969	-2.4768
8.6236	15.385	-0.82078	4.6631
21.832	2.7898	3.0013	-3.291
-7.0343	0.64653	10.253	-2.3119
-16.444	-9.785	-5.7878	-1.4173

TABLE 7
LAYER WEIGHTS FOR THE SECOND TRAINING SET'S NEURAL NETWORK.

		Layer Weights																						
-2.9606	2.2623	3.3407	2.1268	27.558	1.8814	-18.824	-12.109	-0.92695	-0.27381	-3.7446	7.0945	0.52746	0.97115	-0.39393	2.6157	22.212	10.992	-2.2468	1.9261	21.949	-5.3786	-11.485	2.0012	1.2578
2.9804	1.6687	0.97211	0.9137	-0.58727	1.6326	2.1278	-1.8446	-0.79113	1.4479	4.6158	0.65458	-1.5933	5.1735	1.7741	0.59749	-14.215	2.1059	0.66159	1.1401	3.1018	1.2254	-4.5343	0.28572	0.72617
-3.0342	6.139	0.29086	0.5771	-3.5521	-2.4476	-2.0872	-3.1736	-8.7093	-0.74622	0.65014	-3.7176	-3.1646	0.094992	0.3452	0.93747	-0.038714	0.60255	-1.5476	0.20304	-2.9749	0.45631	-0.76982	1.2945	1.8396
-9.7621	-13.878	0.81057	0.94635	0.59297	-4.7997	3.1504	-11.245	12.435	-2.0589	0.71813	-5.8981	3.7079	-0.29702	-0.96937	-0.18008	0.59908	0.80005	-1.2122	0.28043	2.611	0.067595	0.17872	1.2241	-0.051645
3.4	20.022	2.5353	3.1021	10.647	25.515	7.6572	4.1109	5.6752	-3.3888	2.3478	-20.853	-18.382	-2.1062	0.55464	2.3945	-1.1246	5.9263	-1.4413	2.0864	7.9438	-0.73803	-1.191	2.5279	2.3092
5.0553	6.5158	0.53306	0.48512	19.301	11.293	-1.2428	-3.8014	-1.1758	0.15084	-2.1725	-3.9869	0.48029	1.7296	-4.5429	3.5424	27.56	8.405	-4.5795	4.2544	13.154	-0.14912	-2.8648	0.83903	5.1857
-7.2258	2.6895	2.0208	6.3071	-7.0719	-9.6853	0.296	3.339	0.10341	-9.9655	-8.9771	-1.8573	0.059378	4.9439	2.7096	0.91707	24.709	2.1558	-2.2659	1.2572	1.6384	0.64098	-1.94595	2.1962	1.0407
8.3	0.39298	0.42676	1.3404	8.4928	-2.7808	-9.0416	1.6822	-0.19097	-10.909	-8.2688	-0.71807	0.83299	6.1733	3.4137	1.6582	31.113	7.8663	-8.0816	7.7777	9.9837	22.977	-0.94595	2.1962	1.0407
2.4491	0.33951	0.51542	-0.27885	-3.9813	-11.832	0.44218	-0.69854	-0.027719	5.4002	4.3969	-11.5129	0.20379	1.2981	-2.5409	0.25245	26.113	-0.082053	0.23692	0.5367	0.22753	22.079	-15.967	0.10413	0.89928
0.21521	10.233	1.292	1.4381	-29.059	-13.144	-1.949	6.0421	4.0891	-12.305	9.6567	-11.815	8.8949	10.862	2.5746	2.5533	0.2592	-10.374	-2.17	2.1578	0.35033	-1.0638	-0.67295	2.2505	2.5725
7.1231	-23.087	5.238	4.8944	-5.1284	13.9	7.0051	3.4717	19.433	0.094279	2.7204	12.978	0.11365	29.859	0.17681	4.9367	-0.42306	-11.246	-4.2799	4.4585	-4.0353	-0.11324	-1.9119	5.4631	5.3386
1.2643	-1.2381	4.8558	0.73913	-4.5726	-4.466	-0.77079	1.0719	-10.979	3.2719	-1.4676	1.7086	5.0645	3.4523	-11.534	1.5434	0.37186	-5.8642	-0.48633	1.4896	15.324	-1.1801	0.046876	-0.1043	-0.17575
-4.4026	-0.69591	2.5915	2.6985	0.49545	-2.8305	8.8699	-6.4463	-22.112	-11.403	0.68201	-1.4139	-19.906	7.9604	-0.10889	1.3669	-0.80456	6.2181	-2.522	2.352	2.423	-0.48347	-2.536	3.3864	1.977

TABLE 8
BIAS VECTORS FOR THE SECOND TRAINING SET'S NEURAL NETWORK.

B1	B2
12.154	0.75998
-25.13	2.4705
-18.597	0.95916
-29.169	-2.4291
16.602	-3.2451
-25.987	-0.46432
16.92	-6.8776
-14.832	0.23401
11.647	-1.7093
-3.8512	-3.4536
12.109	-6.7669
-32.213	1.8366
-9.5428	-5.5231
17.177	...
11.698	...
0.8226	...
-18.161	...
27.29	...
8.1008	...
1.1608	...
-26.482	...
-29.129	...
-19.65	...
-26.392	...
12.136	...

Fig. 1.— Principal component plot showing the different asteroid classes. From this figure it is clear that the different classes are organized nicely into groups in PC space. This is expected from previous work, and an indication that the neural network's results are accurate.

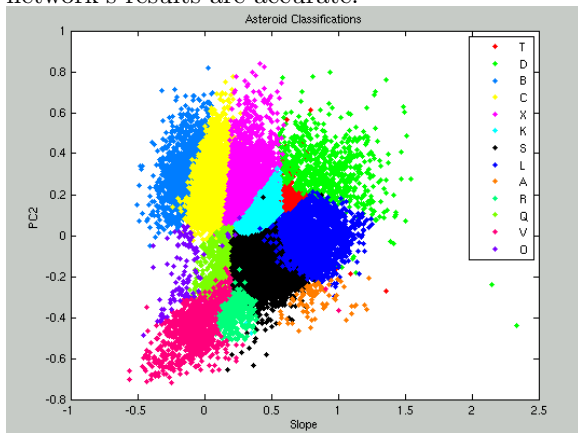


Fig. 2.— Histogram of highest probabilities for each asteroid. 90% of asteroids have a probability of 50% or higher, meaning that the neural network can strongly classify the vast majority of asteroids.

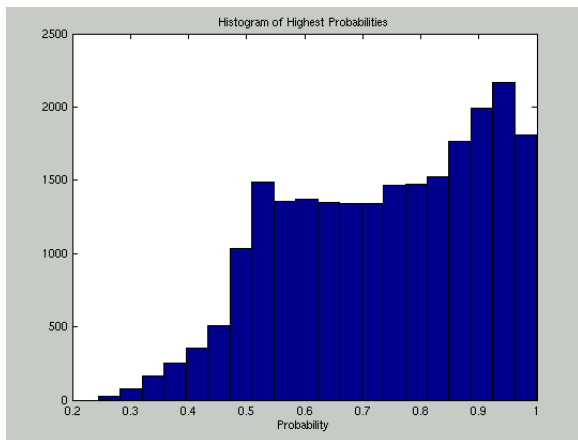


Fig. 3.— Plot of V and R types in orbital element space. Some of the Vesta family asteroids are classified as R's, either due to measurement errors or inherent spectra disparity within the Vesta family.

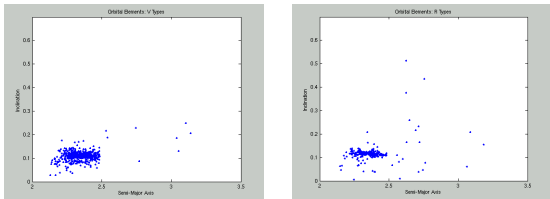
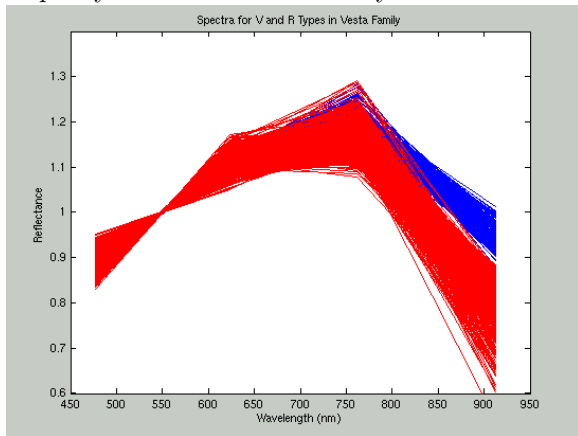


Fig. 4.— Spectra for asteroids classified as V and R types in the core of the Vesta family. The V types are in red, the R types in blue. There is clearly a difference between the two groups of spectra, indicating that there is either a measurement error, or more likely, that there is true spectral disparity within the Vesta family.



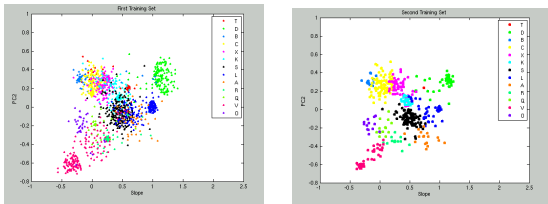


Fig. 5.— Principal component plot of the two training sets. This figure displays the asteroids used in the training sets in principal component space with the different classes differentiated by color. The first training set includes over 1700 asteroids from previously published papers, known families, and asteroids we manually classified are included in this training set. The second training set contained around 600 asteroids that were classified by eye.

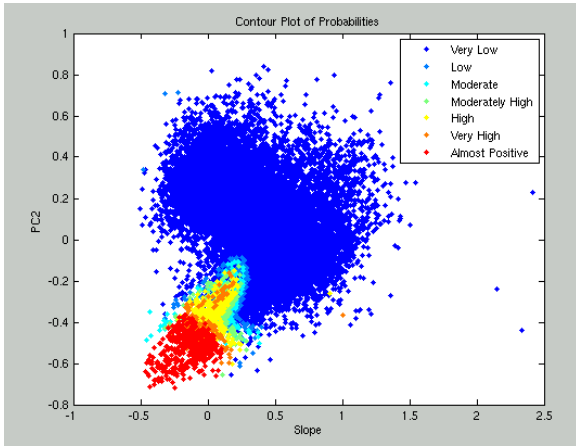


Fig. 6.— Probability contour for V class asteroids. The figure shows the different probabilities the neural network gave for all the asteroids in principal component space. The V asteroids are found in the bottom left corner of the plot, which is expected. Additionally, there are many very strongly classified V-type asteroids in the SDSS data set.

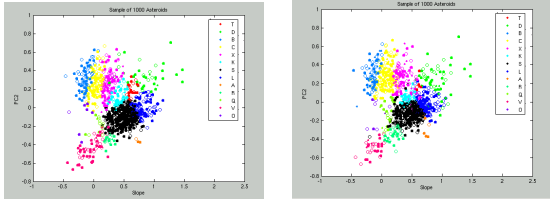


Fig. 7.— Results for a random sample of 1000 asteroids from the SDDSMOC. The different colors represent the different classes, and the different markers show the probability of each classification. Solid markers are in the range of 75% and higher, open markers are 50% to 75%, and the dots are under 50%. On the left are the results for the first training set, and the results for the second training set are on the right. The results are similar with only subtle differences, such as the sharpness of the boundaries and the strength of some classes.

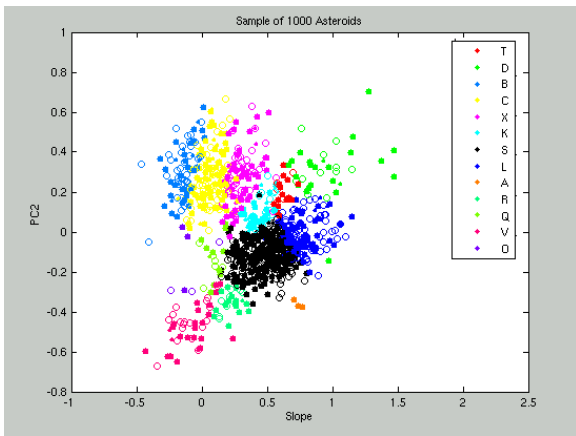


Fig. 8.— Final results for a random sample of 1000 asteroids from the SDSSMOC, using the same color and marker scheme as in Figure 7. While similar to the results from the two training sets, the final results show less sharp boundaries between the classes and a better balance between the strength of the classes.